ORIGINAL ARTICLE

Drivers of marine heatwaves in a stratified marginal sea

Matthias Gröger[1] · Cyril Dutheil[1,2] · Florian Börgel[1] · Markus H. E. Meier[1]

© The Author(s) 2024

Abstract

Marine heatwaves (MHWs) can cause devastating impacts in coastal marine ecosystems, particularly in shallow marginal seas, thereby making the understanding of the drivers of these events of paramount importance. Here, drivers for summer and winter MHWs are explored for the period 1980–2016 in the Baltic Sea, a mid-latitude marginal sea with a permanent haline water-column stratification located on the northwestern European shelf. It was found that summer MHWs are mainly forced by local meteorological conditions over the open water. They are caused by a dominant blocking over Scandinavia promoting anomalous strong shortwave downflux, calm winds, and low vertical mixing with colder sub-thermocline waters. Wintertime MHWs are linked to the advection of warm and moist air originating from the North Atlantic. These air masses lower the oceanic net heat loss at the sea surface primarily in the form of reduced latent and sensible heat losses. Vertical ocean dynamics are also affected during winter MHWs. This study finds a strengthened coastal up- and downwelling due to anomalous strong westerly winds during the time before MHWs culminate in their maximal surface extension.

1 Introduction

Periods of anomalous warm water temperatures can constitute a serious threat for ecosystems (Post et al. 2009; Beger et al. 2014) with cascading effects into higher trophic organisms such as marine mammals and seabirds (Huntington 2009). Marine heatwaves (MHWs) are expected to occur more frequently and with greater intensity along with global warming (Qiu et al. 2021; Li and Donner 2022; Benthuysen et al. 2020; Hobday et al. 2016; Oliver et al. 2018). The Baltic Sea is a prominent example how anomalous warm waters can negatively influence the marine ecosystem and fishery economics. In recent years, the western Baltic Sea frequently experienced anomalous warm winters, which caused extraordinary early hatching of herring larvae in spring, resulting in a dramatic and potentially irreversible decline of the herring population (Polte et al. 2021). Moreover, there is strong evidence that the economically most important fish species in the Baltic Sea, i.e. cod has reached a tipping point because current exploitation levels do not account for the warming water masses along with climate change (Möllmann et al. 2021; Receveur et al. 2022). Moreover, in 2018, when central Europe was impacted by an extraordinary strong atmospheric heat wave (Kueh and Lin 2020) the Baltic Sea experienced the largest hypoxic area throughout the worlds coastal seas (Meier et al. 2021; Krapf et al. 2022). Consequently, the recent extraordinary warm years strongly stimulated scientific research as well as the public awareness concerning MHWs in the Baltic Sea region (Suursaar 2020; Goebeler et al. 2022; Möllmann et al. 2021).

High latitude regions like the Arctic and the Baltic Sea have warmed up significantly faster than other world regions during the last four decades (Rantanen et al. 2022; Meier et al. 2022a, b) and thus increased the risk for MHWs. Furthermore, their perennial haline stratification limits the downward heat transport to ocean interior by mixing. However, local driving mechanisms for MHWs in stratified sub-polar regions are not yet fully understood and moreover, may be diverse according to the specific oceanographic and climatic conditions of the region and with respect to the season. For example, diminishing sea ice may lead to an increased absorption of solar radiation but on the other hand, can promote an increased heat flux out of the ocean when more open seawater is exposed to the cooler atmosphere in particular during the cold season. A first general framework for analyzing the broad-scale

✉ Matthias Gröger
 matthias.groeger@io-warnemuende.de

1 Department of Physical Oceanography and Instrumentation, Leibniz Institute for Baltic Sea Research Warnemünde, Rostock, Germany

2 MARBEC, University of Montpellier, CNRS, Ifremer, IRD, Sète, France, Montpellier, France

driver of MHWs was given in Holbrook et al. (2019) who found that MHWs often correlate with distinct phases of binary climate modes such as the North Atlantic Oscillation (NAO) or the El Nino Southern Oscillation.

So far, MHWs have been robustly evaluated and categorized on a global scale for the historical period and in future climate change projections in the framework of the Coupled Model Intercomparison project (Qiu et al. 2021) as well as in global hindcast studies or reanalysis data (Vogt et al. 2022). However, global assessments should not be rendered without caution on coastal seas which include many local processes not accounted for in global models. Regional high resolution studies are however still rare (Behrens et al. 2022) and the relevant processes triggering MHWs varies with location and thus, can not be generalized.

The Baltic Sea, a marginal ocean basin located on the NW European shelf, is an excellent natural laboratory to study ocean–atmosphere interactions triggering MHWs. The Baltic Sea region is among the fastest warming oceans in the World (Meier et al. 2022b; Christensen et al. 2022; Dutheil et al. 2022) and a prominent example for record breaking temperatures (Meier et al. 2017). It is an estuarine sea with a surface area of approximately ∼ 420,000 km^2 and a water body of ∼ 20,000 km^3 with no direct connection to the open ocean (Fig. 1a). Oceanographic conditions range from almost fully marine in the southwest to nearly limnic conditions in the north. Inflow of salt water is restricted to small channels with a maximum width of 200 m and up to 10 m depth between Denmark and Sweden. Sporadic saltwater inflows from the adjacent North Sea maintain a permanent haline stratification with a strong halocline at depths ranging
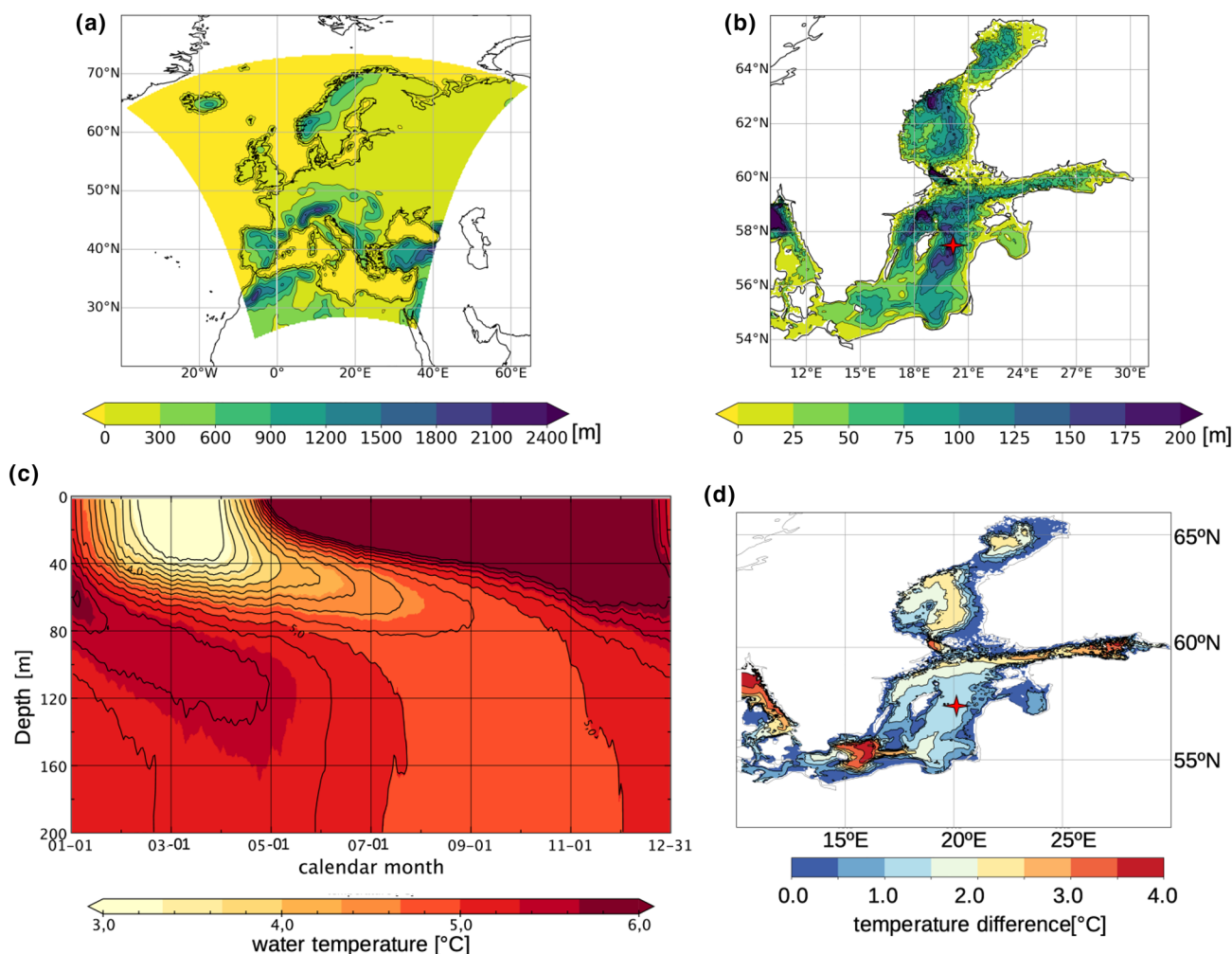
Fig. 1 **a** RCA4-Euro-Cordex model domain including land elevation. **b** Ocean bathymetry of the ocean model for the Baltic Sea. Not shown is the extention over the North Sea. The red star indicates the monitoring station BY15. **c** Modelled multi-year (1980–2016) average seasonal cycle of water temperature profile at BY15. Note the temperature scale is cut off above 6 °C and below 3 °C in order to visualize the vertical thermal layering around the halocline. **d** Maximum winter (DJFM) temperature in the water column expressed as the difference to the surface temperature. Shown is an average over the years 1980–2016

between 60 and 80 m. The presence of sea ice is restricted to the cold season.

For the analysis of atmospheric drivers and ocean feedbacks, the days or weeks during which the MHWs develops are essential. Since the duration of MHWs is usually shorter than seasonal atmospheric modes (such as NAO), this study explores the role of synoptical weather patterns in the genesis of MHWs using the concept of weather regimes (Grams et al. 2017).

Besides the atmospheric preconditioning, MHWs can be further shaped by internal ocean dynamics that control the vertical heat exchange. In particular the role of the mixed layer thickness has been emphasized recently (Elzahaby et al. 2022). In addition, a concise feature of haline stratified seas like the Arctic and the Baltic Sea is the presence of a warm deep-water body overlain by a cold halocline surface layer. In the Baltic Sea such conditions are restricted to the cold season and are primarily the result of summer to winter vertical heat distribution: Intense solar radiation leads to a rapid warming of the surface layer and establishes a strong thermocline in June (Fig. 1c). Convectives mixing, and also wind mixing with the start of the storm season in autumn, export warm surface waters to deeper layers. Subsequent surface cooling over the winter months leads to incorporation of warm sub-halocline waters in the water column (Gröger et al. 2022b). As a result, the water temperature found around the halocline can be up to 4 °C higher than at the surface (Fig. 1c, d). Overall, in the Baltic Sea, the halocline barrier leads to the characteristic feature with a cold intermediate layer in the warm season (e.g. Dutheil et al. 2023) and the presence of a deep warm water body in winter with a temperature maximum between 60 and 100 m depth (Fig. 1c). The role of deep warm water reservoirs as a potential heat source for MHWs has not been studied so far neither in the Baltic Sea nor elsewhere.

Finally, the Baltic Sea's marked halocline layer, it's intense air-sea thermal coupling (Gröger et al. 2015), the presence of sea ice, and its strong sensitivity to climate warming make this sea an ideal laboratory exemplary for sub-polar halocline marginal ocean basins.

2 Methods

2.1 Coupled ocean–atmosphere model

The hindcast data used in this study were produced with the coupled ocean–atmosphere model RCA4-NEMO (Gröger et al. 2015; Dieterich et al. 2019) which has been forced with ERA-Interim reanalysis data (Dee et al. 2011) for the period 1980–2016.

The atmospheric component is the Rossby Center regional Atmosphere model (RCA, Samuelsson et al. 2011).

The model grid has a horizontal resolution of ∼ 24 km and vertically resolves the atmosphere by 40 levels. At the lateral boundaries RCA4 was driven by 6-hourly temperature, humidity, and wind components derived from ERA-I. At the lower boundary ECOCLIMAP (Champeaux et al. 2005) was used to calculate energy and mass fluxes at the land-sea interface. For the open ocean of the Atlantic, the Arctic, and Mediterranean ERA-SST and sea ice fields were prescribed to calculate air-sea fluxes. For the North Sea and Baltic Sea, a 3D ocean general circulation model based on Nucleus NEMO-3.3 (Madec et al. 2017) was interactively coupled to RCA. NEMO communicates SST, sea ice, temperature, ice albedo, and sea ice fraction (Gröger et al. 2015). NEMO receives mass and energy fluxes derived from RCA and prognostically calculates water temperature and salinity, sea level, and ocean currents. NEMO is set up with a horizontal resolution of two nautical miles and resolves the water column by 56 levels, which range in thickness between 3 m at the surface, and up to 22 m near the seabed. The coupling time step with RCA4 is 3 h. At the northern and western lateral boundary to the North Atlantic sea surface height (SSH) was used to calculate volume in- and outflow. The SSH variations, and the temperature and salinity profiles along the open boundaries were derived from the ECMWF ocean reanalysis system ORAS4 (Balmaseda et al. 2013) and are modulated by 11 tidal components. Further details on RCA4-NEMO, the interactive air-sea coupling and comprehensive model validations are available from the literature (Gröger et al. 2015, 2021; Dieterich et al. 2019). The model has been used in numerous previous regional climate studies in Europe (Gröger et al. 2019, 2021, 2022a; Dieterich et al. 2019; Meier et al. 2022a, b; Wåhlström et al. 2020, 2022).

2.2 Definition of marine heatwaves

MHWs are defined and categorized according to Hobday et al. (2016, 2018):

From the multi-year (1980–2016) daily SST time series:

1. The calendar-day of the year (DOY, hereafter) mean climatology (1979–2016) is calculated within an 11-day window centered around the respective DOY.
2. The DOY 90th percentile is calculated using the same window. No further running 31 day window smoothing was applied on the resulting DOY 90th percentile.
3. The difference (2) minus (1) is calculated.
4. Multiples of (3) are used to define thresholds for different the MHW categories for every calendar day and every grid cell.
5. The simulated daily SST time series (1980–2016) is evaluated. A category I MHW day is defined if the difference between the simulated daily mean SST minus (1) exceeds (3). A category II heatwave day is defined if the

difference between the simulated daily mean SST minus (1) exceeds (3) by a factor of 2 and so on.

6. Tor every day, the total area extent (km²) of the ocean surface is calculated that was categorized as MHW.

7. Finally, for each year the seasonal maximum MHW extent for summer (JJASO) and winter (DJFM) is calculated.

The calculation of daily percentiles and average daily climatologies was done using the climate data operators toolbox (Schulzweida 2023).

2.3 Derivation of composite anomalies

Composite anomalies are created as:

1. The calendar date of yearly maxima of respectively summer (JJASO) and winter (DJFM) MHW extent are extracted (Day Of Maximum Marine Heat Wave Extent = DOMHWE hereafter) resulting in 37 calendar dates (1980–2016) for summer and winter.

2. For each calendar date the preceding 30, 15, and 5-day periods are gathered resulting in a total sample size of 37×30, 37×15, and 37×5 days.

3. The composite mean climatology is then multi-year (1980–2016) average of the 37 respective 30, 15, and 5-day periods

4. A reference climatology is defined by the multi-year (1980–2016) average of the entire summer (JJASO) and winter (DJFM) season.

5. Composite anomalies were built by subtracting the composite mean climatology from the reference climatology.

For the considered variables sea level pressure (SLP), 2 m air temperature (T2m), 10 m wind speed, ocean mixed layer thickness (MLD), downward solar radiation (DSWR), thermal radiation (DLWR) the multi-year mean seasonal cycle was subtracted before processing.

Significance

A bootstrapped signal-to-noise ratio was performed to test the significance of the composite anomalies. The noise was estimated from in total 100 iterations where the calendar dates and hence, the preceding 30, 15, and 5-day periods were chosen randomly and not defined by the annual maximum MHW extent. The composite anomalies were considered significant when the signal to noise ration exceeded two standard deviations.

2.4 Classification of weather regimes

In order to define characteristic weather patterns we classified meteorological conditions by applying the concept of

(Grams et al. (2017)). While it is not yet clear whether or not WRs represent real modes of physical variability (Hochman et al. 2021), they are a useful tool to categorize atmospheric patterns on a sub-seasonal scale (Fereday 2017). The method is based on the z500 geopotential height fields to define eight distinct classes of weather regimes (Fig. 2). An empirical orthogonal analysis is carried out in which the first 7 leading empirical orthogonal functions (EOFs) were retained. This results in seven different weather regimes which together explain ~ 65% of the z500 geopotential height variance plus one "no regime" class for the residual (Fig. 2).

The detected WRs analyzed in the time preceding the DOMHWE. We focus on a period of T = 25 days before DOMHWE. Then each of the 25 days were assigned to the specific WR that prevailed at this time. After that, we calculated for all the 25-day periods the occurrence frequency (F) of each specific WR.

$$F(k) = \frac{\sum_{j=1}^{N} Length(D(j) \cap R(k))}{Length(R(k))} \times 100 \tag{1}$$

D(j) = all T = 25 days before a MHW with j the number of MHW. R(k) = all days (1980–2016) associated to a WR with k from 1 to 8

We then subtracted the climatological frequency of WR occurrence (determined over the whole 1980–2016 period) from F(k) to calculate an anomaly (A). Thus, A(k) represents the deviation of WRs occurrence frequency before the triggering of a MHW event compared to the climatological mean state.

$$A(k) = F(k) - \frac{Length(R(k))}{M} \times 100 \tag{2}$$

In addition, we also varied the length of period T before the MHWs from 10 to 40 days to estimate the uncertainty related to the choice of this parameter.

3 Results

3.1 Variability of heatwave extent

We investigated the atmospheric conditions that promote MHWs during their formation. Because of the higher thermal inertia of the ocean compared to the atmosphere, MHWs can still exist when favorable atmospheric conditions already vanished. We therefore distinguish a formation phase and a decomposition phase of MHWs and roughly separate the two phases by the calendar day when the respective MHW reaches its maximal extent at the water surface (DOMHWE). Summer and winter MHWs are analyzed separately to account for the converse thermal layering of the water column between winter and summer (Fig. 1c) as well as for the
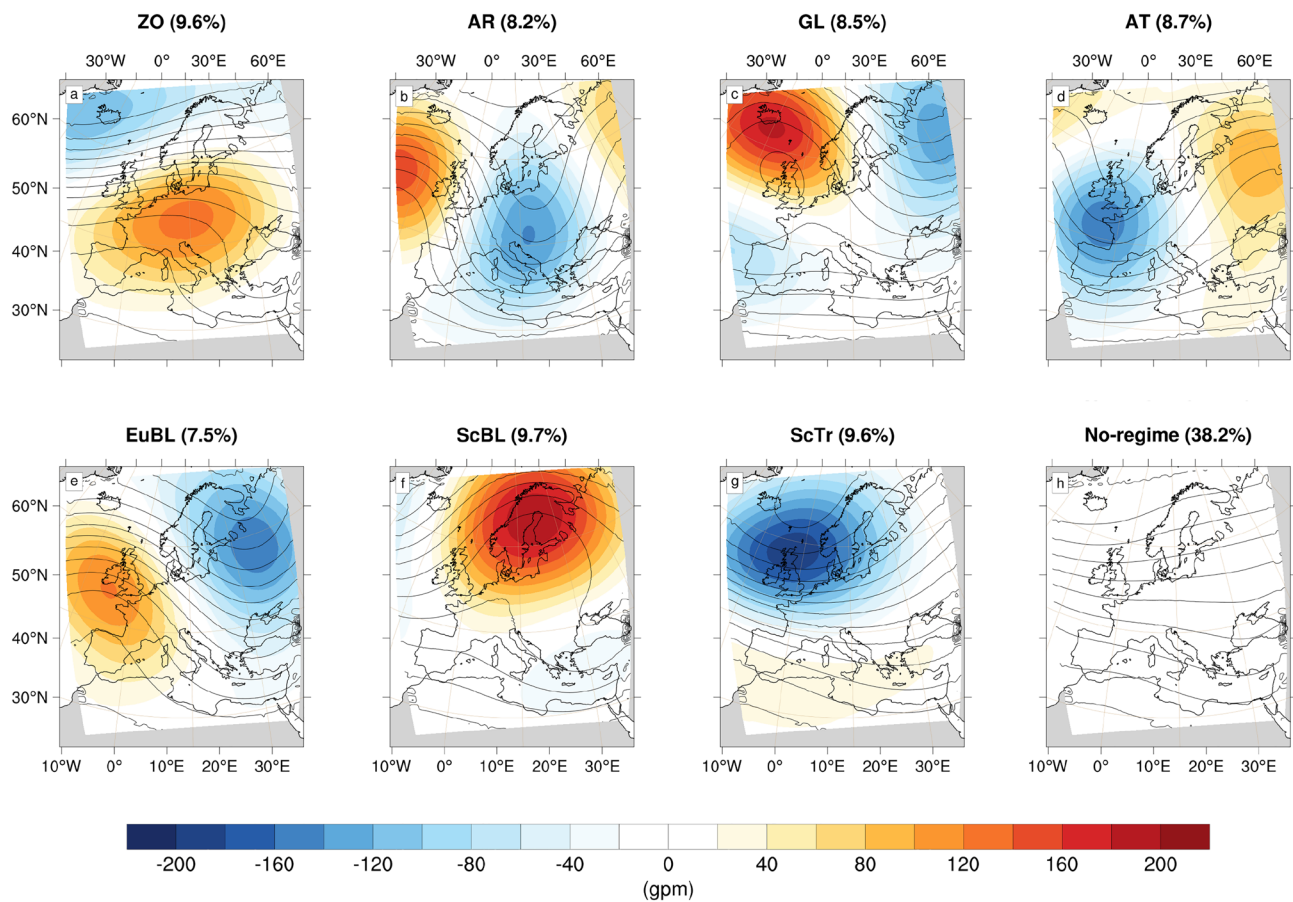
Fig. 2 Atlantic-European weather regimes diagnosed from the regional atmosphere model RCA4. 500 hPa geopotential height anomaly (shading, in geopotential meters), and mean absolute 500 hPa geopotential height (contours, every 40 geopotential meters) for all days attributed to one of the 7 weather regimes (**a–g**) and to no regime (**h**). *ZO* zonal regime, *AR* Atlantic Ridge, *GL* Greenland Blocking, *AT* Atlantic Trough, *EuBL* European Blocking, *ScBL* Scandinavian Blocking, *ScTr* Scandinavian Trough, *NoRe* no regime. The regime frequencies are indicated in parenthesis

opposite direction of net heat fluxes at the air–sea interface. For our purpose, we define the summer season from June to October when a thermocline effectively separates the thin warm surface layer from colder waters below. The winter season is defined from December to March when the Baltic Sea is well mixed down to the halocline separating colder surface waters from warmer sub-halocline deep waters.

The monthly mean variability of the MHWs surface extent together with the summer and winter daily maximum extent were analyzed (Fig. 3). Over the 37-year long period, we find several events with an extraordinary large monthly mean extent of > 300,000 km^2 (or 3/4 of the total area). Most of these events occur in summer when the MHW extent is generally larger than in winter. Noteworthy is an apparent alternation of periods with predominantly low extents (e.g., before 1990 and periods when extents are larger (e.g., early 90ies, Fig. 3a). The frequency and duration of MHWs (Fig. 3b and c) can have a large impact for the life cycle of higher trophic species. For example the

temperature window for the spawning of Baltic Sea Herring could be shifted to earlier or later in the year during long lasting anomalous warm temperatures, which in turn, can have a big impact on its reproductive success (Polte et al. 2021). The average MHW duration varies between ~6 and 22 days (Fig. 3c) which lies in the range of typical weather systems moving over Europe.

3.2 Meteorological conditions promoting marine heatwaves

We here analyze the period 1980–2016 which encompasses 37 complete summer (JJASO) and 36 complete for winter (DJFM) seasons. In order to explore the environmental conditions that drive these extended MHWs, we analyze the meteorological conditions during the time before the DOMHWE. In particular, we analyze three different time periods:

Fig. 3 **a** Monthly mean spatial extent of MHWs from the hindcast simulation. Yellow and red filled curves denote moderate and strong MHW classes according to Hobday et al. (2018). The triangles connected by the blue and purple lines indicate the calendar day of the yearly seasonal maximum extent for the respective season (blue = winter, purple = summer). **b** Average frequency of MHWs. **c** Average duration of MHWs (blue winter, red = summer)
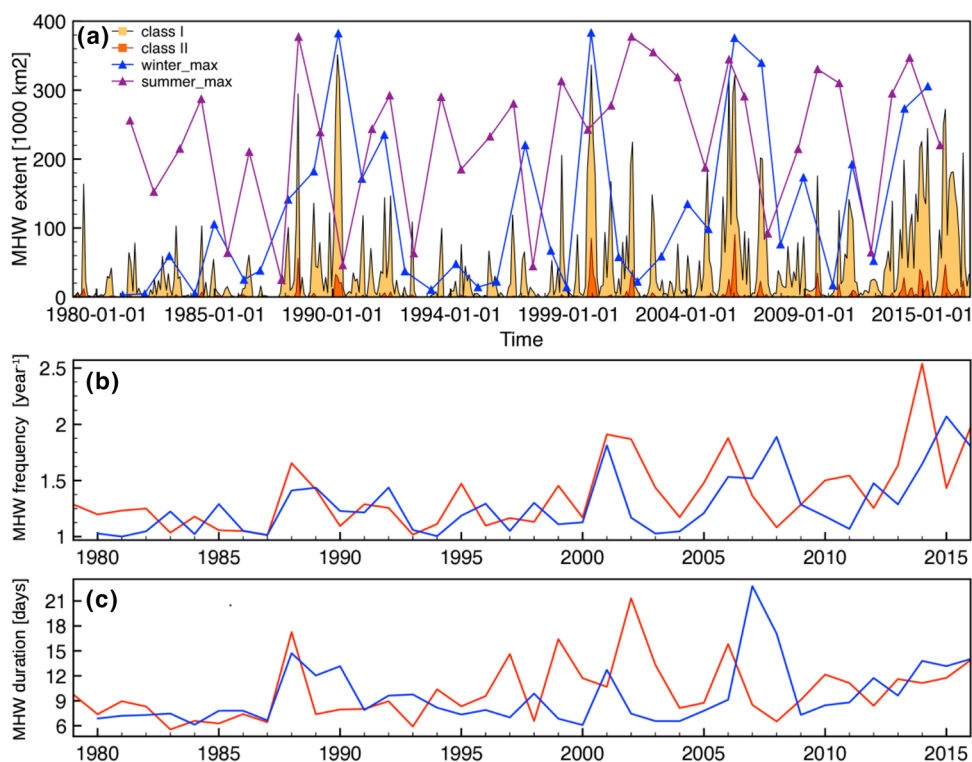
1. a long-term period covering the preceding 30 days which reflect monthly mean conditions before the DOMHWE,
2. a mid-term period of 15 days roughly depicting the range of synoptical variability, and
3. a short-term period of 5-days reflecting the culmination phase right before the DOMHWE.

Since our analysis revealed consistent patterns over all considered periods, we here show only the results for the mid-term period and provide the long-term and short-term periods with the Suppl. Mat. S1.

3.2.1 Summer marine heatwaves

Figure 4 displays anomalies of key variables averaged over the mid-term period. The dominant pattern is a positive sea level pressure (SLP, Fig. 4a) anomaly over Scandinavia which is accompanied by an anomalous strong downward solar radiation (Fig. 4e). This leads to an enhanced heat absorption in the upper water layer of the entire Baltic Sea. The anomalous high SLP conditions in turn, are associated with a positive near surface air temperature anomaly (Fig. 4b) and sustain anomalous low wind speeds over the open sea areas (Fig. 4c). This pattern promotes a persistent stable atmospheric boundary layer as any instantaneous wind event would induce a strong upward mixing of colder sub-thermocline waters which increase the static stability again and so negatively feed back on wind speeds (Gröger

et al. 2015). In turn, the reduced wind speeds translate in generally diminished vertical water mixing (Fig. 4d) closing the negative feedback loop. As a consequence, cold sub-surface waters are effectively thermally decoupled from ocean surface during summer MHWs.

3.2.2 Winter marine heatwaves

Meteorological conditions that trigger winter MHWs are marked by a dipole pattern with anomalous low SLP over the North Atlantic and high SLP over southern Europe (Fig. 4f). As a result the meridional pressure gradients are increased and in line with this, wind speeds are enhanced (Fig. 4g). Hence, along with the stronger winds, warm air masses from the Atlantic are advected towards northern Europe where a positive air temperature anomaly develops (Fig. 4h). This coincides with anomalous high downward thermal radiation (RDLS hereafter, Fig. 4j). These conditions are consistent with the positive phase of the NAO. Hence, the higher RDLS and warmer air temperatures effectively reduce the wintertime oceanic heat loss at the air-sea interface. In addition, higher wind speeds increase the momentum transfer to the sea which exerts a more efficient mixing of surface waters with warm deep waters. All this feeds back positively to the SST and thus supports the development of MHWs.

Summer MHW composites
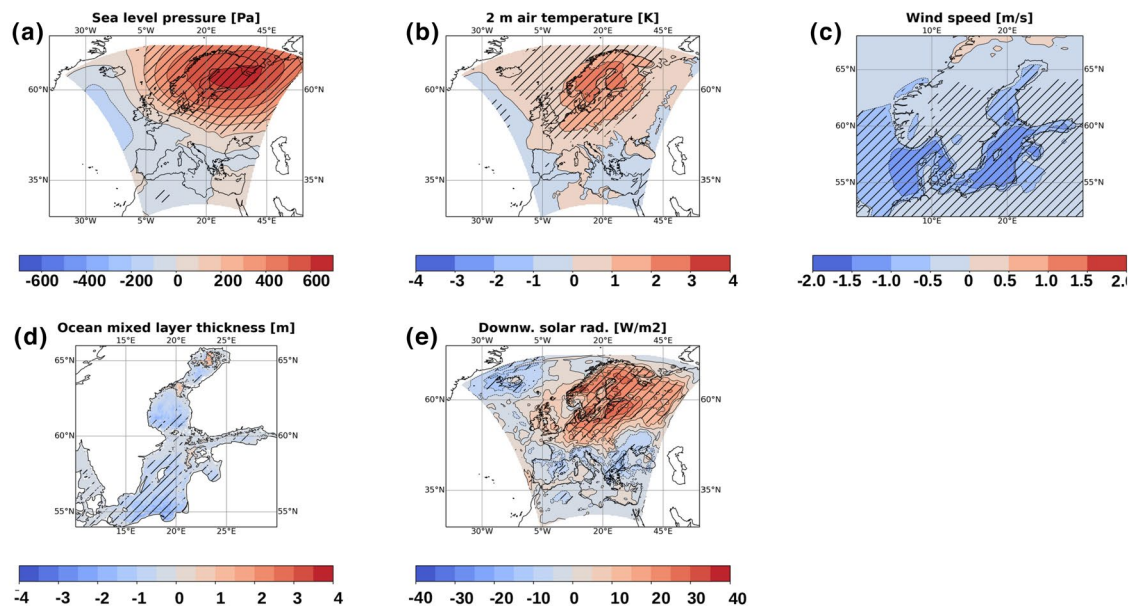
Winter MHW composites
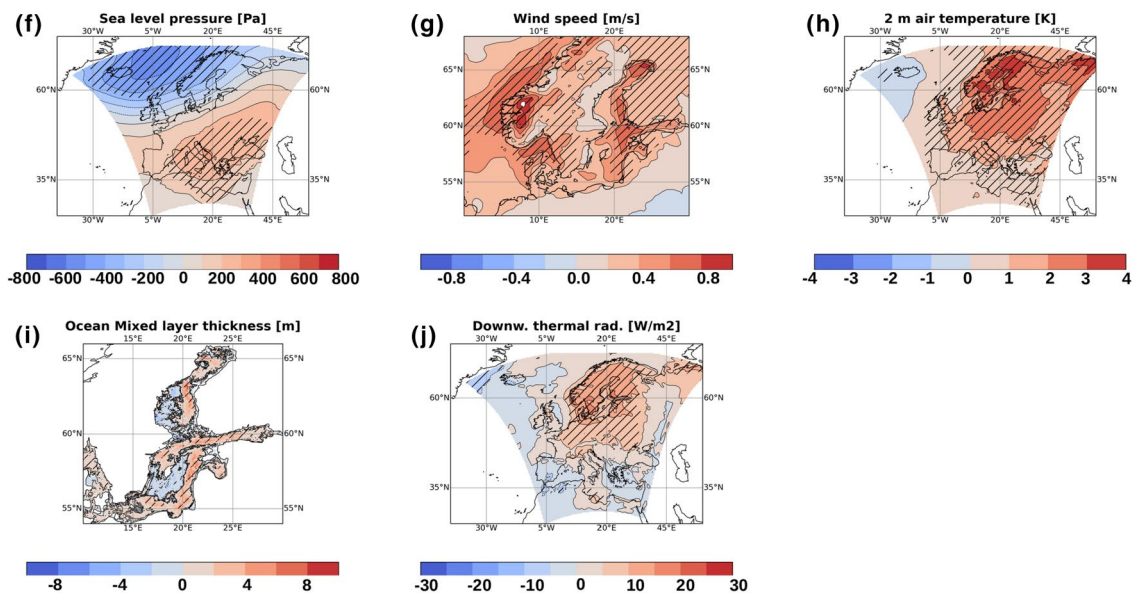
Fig. 4 Summer composite anomalies for **a** sea level pressure, **b** near surface air temperature, **c** wind speed, **d** ocean mixed layer thickness, and **e** downward solar radiation. The anomalies represent mean condi-

tions over the last 15 days before the day of maximum MHW extent. Areas where the signal-to-noise ratio exceeds two standard deviations are hatched

3.3 Weather regimes and marine heatwaves

So far, we identified the local atmospheric mean conditions forcing MHWs for the winter and summer season. Next we address the question if the identified mean conditions were the result of mainly stochastic variability, or if dominant

patterns of recurring WRs exist that sustain the specific local conditions favorable for MHWs over the Baltic Sea and before the DOMHWE (Fig. 4).

Our results reveal a clear dominance of Scandinavian Blocking (ScBL) during summer and the Zonal Regime (ZO) during winter (Fig. 5). We further compared the

Fig. 5 WR frequencies preceding MHW events in the Baltic Sea. The period considered for the color bars is of 25 days before a MHW event, and the error bars represent the maximum and minimum of this deviation in a window comprised between 10 and 40 days before a MHW event. These deviations are calculated for the MHW classes Moderate and Strong. The deviation are calculated by season **a** summer JJASO and **b** winter DJFM. WR acronyms are explained in Fig. 2
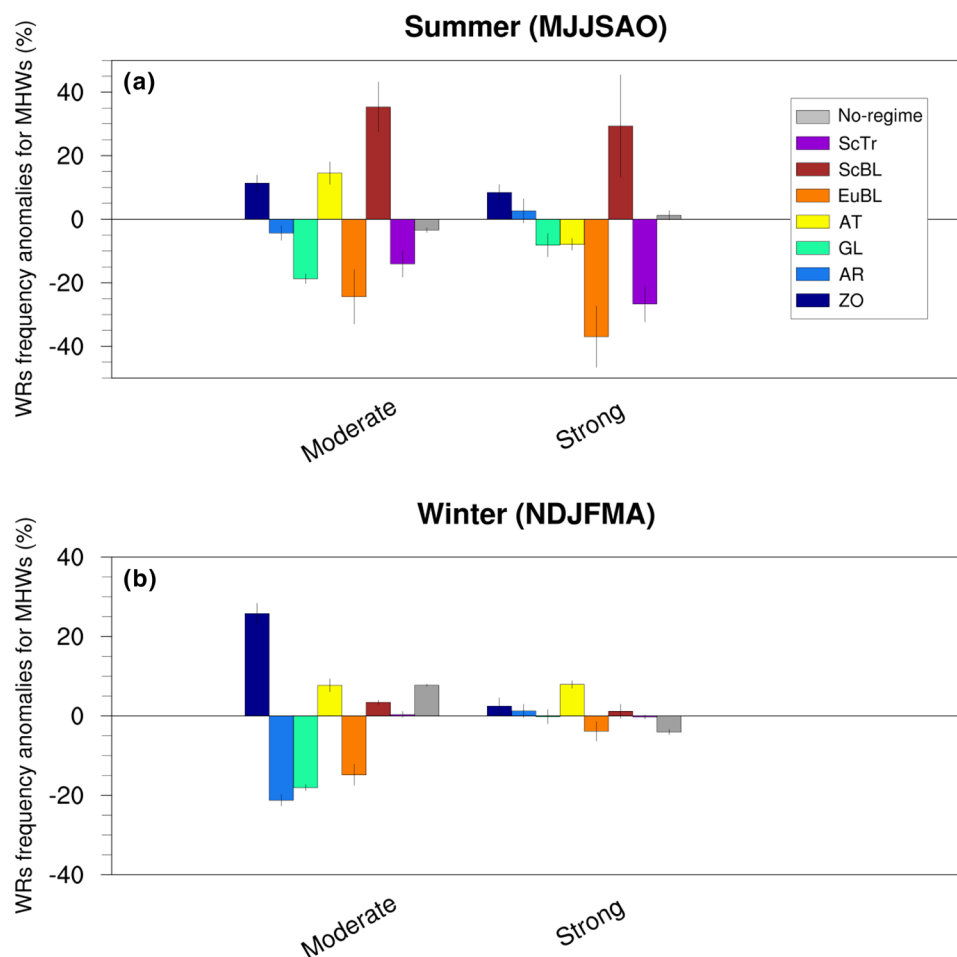
specific weather conditions that prevail under the identified ScBL and ZO regimes (Suppl. Mat. S2, Fig. S3) with the composites representing average conditions before the DOMHWE (Fig. 4). It is clearly demonstrated that the WR anomalies in SLP, T2m, MLD, DLWR, and DSWR (Suppl. Mat. S2, Fig. S3) exhibit the same spatial pattern seen in the mean composite anomalies (Fig. 4). Thus, the high consistency between the two independent methods indicates that the identified WRs ScBL and ZO are the main driver of MHWs in the Baltic Sea.

With regard to the strong the events of MHW category II (Fig. 5, right panel) no WR is likely to occur >10%. The low likelihood is probably linked to the small number of strong events, which hampers robust statistics. It is likewise possible, that strong winter upwelling events, which often occur along the coasts, well-up warm sub halocline waters from the deep warm water body causing temporary very high SST anomalies of short duration and limited surface extent. It is plausible that such small events can occur independently from larger scale WRs.

By contrast, most other WRs are neither under- nor over-represented before the DOMHWE or show even negative

anomalies (e.g. Greenland Blocking, European Blocking, Fig. 5) indicating a lower risk for MHWs to develop. Notably, European Blocking and the Scandinavian Trough WRs are characterized be anomalous low SLP over eastern Europe (Fig. 2) and central Europe respectively. Such conditions of low pressure are associated with cloudy and rainy weather promoting unfavorable conditions for MHWs in summer.

3.4 Role of heat fluxes at the air-sea interface in winter

Our results reveal that the mechanisms leading to extended MHWs completely differ with respect to the warm and cold seasons in the Baltic Sea. Thus, we can distinguish basically two classes of MHWs with respect to their forcing. Class 1 MHWs are primarily driven by prevailing local meteorological conditions and are found during the warm season. They are marked by anomalous high radiative heat absorption from the atmosphere. The presence of the thermocline hampers the exchange with the colder deep water.

Class 2 MHWs occurs during winter and are controlled by external heat supply from the North Atlantic. In this case

basically two heat sources can promote surface warming during the genesis of MHWs. (1) Advective transport of warm air masses from the North Atlantic and, (2) mixing with warmer waters from the deeper warm water body which is driven by the anomalous strong westerly wind field (Fig. S3b). Compared to summer, this points to a more complex situation with regard to the energy flow in winter. We therefore investigate heat fluxes from the two sources in more detail.

We start with an analysis of the anomalous heat fluxes at the ocean's surface during MHWs (Fig. 6) compared to the climatological reference. Figure 6a indicates the total

oceans' heat loss at the air-sea interface is almost everywhere strongly reduced during the 15 days before the DOMHWE. The signal is general weaker along the coasts and in the westernmost Baltic (Kattegat) which likely reflects the lower heat content in these shallow regions whereas the heat loss is stronger reduced in deeper open ocean regions like e.g. the eastern central Baltic (Gotland Basin). However, the lowest signal is found in the northernmost basin (Bothnian Bay) where the signal remains below the noise level, and thus, is not distinguishable from the natural variability. In the northernmost bay around 65 °N negative values indicate even an enhanced heat loss. In this area usually
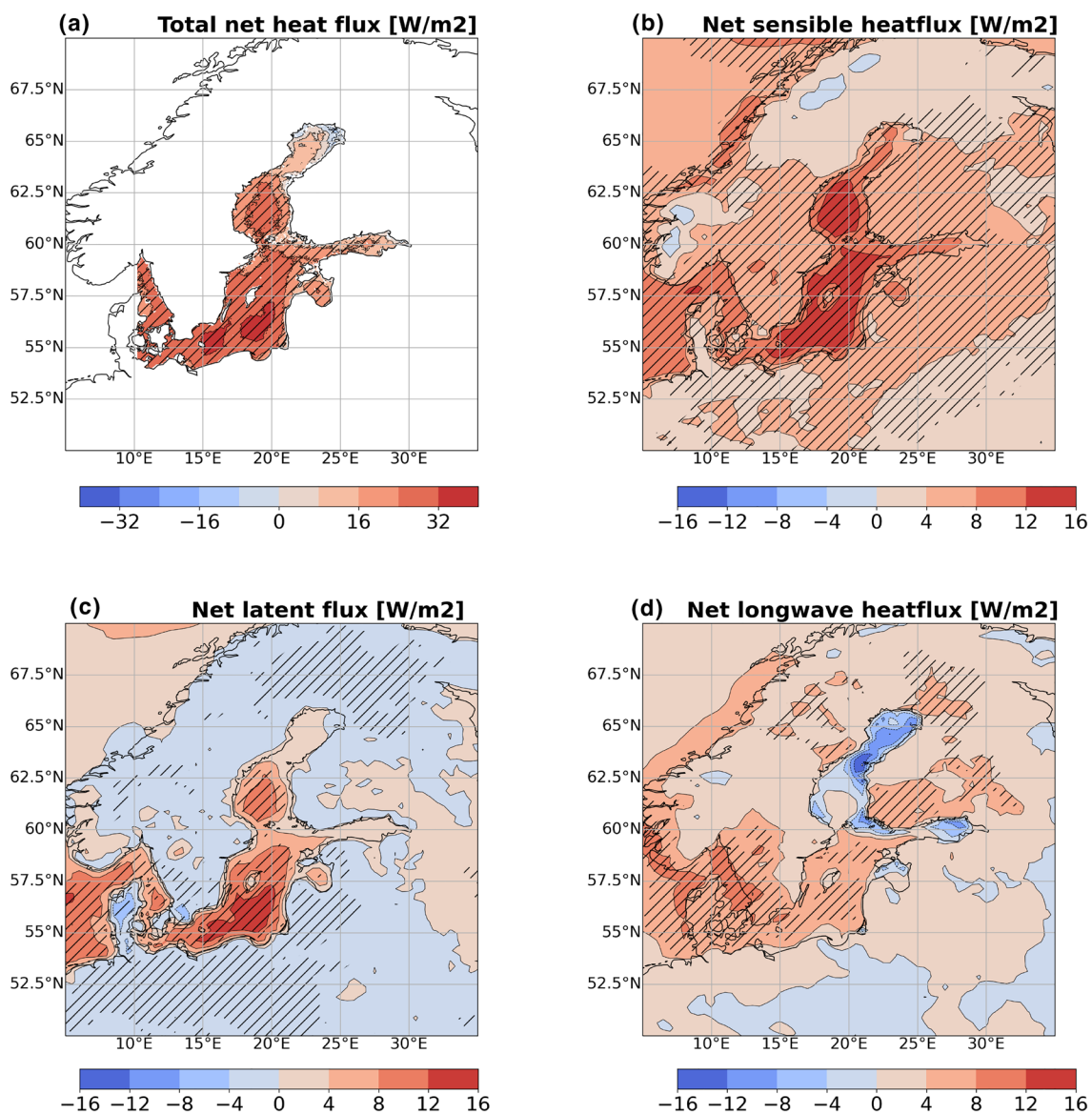
Fig. 6 Analysis of net heat fluxes averaged over the last 15 days before the DOMHWE during winter. **a** total heat flux diagnosed from the ocean model, **b** sensible heat flux, **c** latent heat flux, **d** longwave heat flux. Displayed are anomalies over 15 days before the DOM-HWE compared to the climatological reference. Areas where the signal to noise ratio exceeds two standard deviations are hatched. Averages are shown over 36 MHWs. Positive (= red) fluxes indicate a reduced heat oceanic loss to the atmosphere

stable ice conditions prevail, but during MHWs ice cover is anomalous low which promotes an enhanced heat flux to the atmosphere.

Overall, the reduced oceanic heat loss is mostly reflected by the strongly reduced sensible heat flux to the atmosphere (Fig. 6b). The found high gross influx of thermal radiation shown in Fig. 4j is mostly compensated by a corresponding outgoing thermal flux, so that thermal radiation contributes only a minor portion to the total anomalous net heat exchange during MHWs (Fig. 6d). Moreover, in the northern Baltic Sea the anomalous low sea ice cover and decreased ice thickness promotes an increased thermal radiative heat flux out of the ocean.

In the southern Baltic Sea a significant portion of the reduced heat loss is given by latent heat fluxes (Fig. 6c). This is related to the fact that the ZO regime leads to an enhanced advection of wetter air masses from the North Atlantic which increase the near surface humidity. The effect of elevated humidity on the dew point is larger than the effect of the higher air temperature in parallel, which ultimately results in lower evaporation and reduced latent heat flux during MHWs.

3.5 Ocean energy dynamics during winter marine heatwaves

The reduced heat loss to the atmosphere during winter MHWs has of course an impact on the vertical energy flow in the oceans' interior. Contrary to summer when a strong thermocline effectively decouples the warm surface layer from the cold deep water, during winter strong winds promote vigorous mixing with the warm deep water body (Fig. 1c and d). To investigate this, we calculated linear trends of the mixed layer thickness over the 15 days before the DOMHWE (Fig. 7a). The trends are almost everywhere positive indicating that turbulent mixing accelerates. However, the trends do nowhere exceed 0.5 m/day corresponding to a increase of the MLD by not more than ∼ 7.5 m. In addition to turbulent mixing, large-scale advective mixing is affected. Due to the anomalously strong westerly wind regime the overall water mass circulation is enhanced. To demonstrate this, we analyze the zonal overturning function 15 days before the DOMHWE and compare it to the reference state (7b). In agreement with the prevailing westerly wind regime the dominant feature is the E-W clockwise overturning cell. The maximum overturning function found at around 15 °E and 20 m depth is increased by 48% before the MHW culminates. This increase is mainly wind driven by anomalous downwelling at the eastern and southern coasts as well as upwelling along the western coast. This is well reflected by the deepening of the mixed layer in the east and a thinning in the west (Fig. 4i).
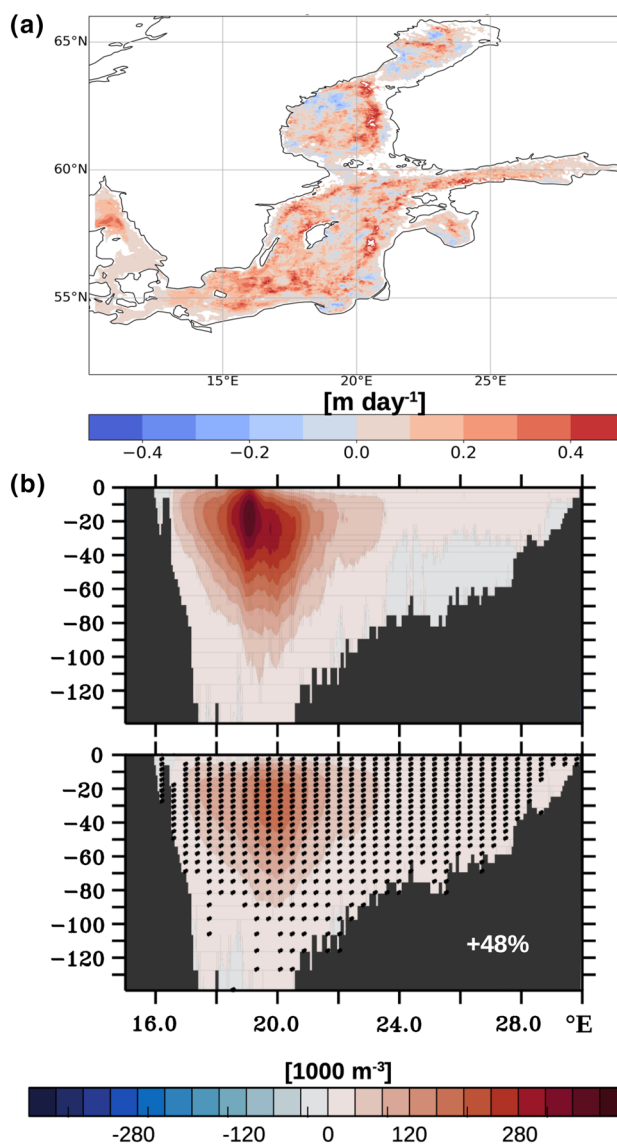
Fig. 7 a Winter linear trends of mixed layer thickness calculated over the last 15 days before the DOMHWE. **b** Top row: winter climatological mean zonal overturning function north of 56 °N. Positive values indicate clockwise circulation. Bottom row: Difference to the climatological mean circulation during the 15 days before the DOMHWE. White number denotes the relative increase of the maximal overturning compared to the climatological reference. Areas where the signal to noise ratio exceeds two standard deviations are hatched

4 Discussion

There are some aspects associated with our method that should be considered. The methodological separation of MHWs into a formation and a declining phase is based on the maximal spatial extension of the MHW. The maximal extension however, must be considered the net result of local increases and losses of daily MHW extent that will take place in parallel in different regions of the Baltic Sea.

Likewise, the onset of a MHW will differ from region to region. Therefore we found the analysis of meteorological conditions backward in time from the DOMHWE a reasonable approximation to investigate the atmospheric conditions that force MHWs. Other proxies to identify a MHW formation phase may be useful as well, e.g. diagnosing the time span of maximal increasing rates of daily MHW extent etc, but were not tested in this study. That said, it is clear that favorable WR may still exist after DOMHWE though not being sufficient to increase the total MHW extent further. Moreover, due to the oceans inertia and effective heat capacity the MHW can still exist long after the DOMHWE, while meteorological condition may already provide conditions that support the decline of MHW.

The identification of two distinct WRs respectively forcing winter MHWs (ZO) and summer MHWs (ScBL) demonstrates the theoretical possibility to predict MHWs in the Baltic Sea a few weeks or months in advance simply by analyzing meteorological data such as the geopotential height of 500 hPa. In fact, efforts for the operational forecast of WR are currently pursued by the European Center for Medium Range Weather Forecasts (e.g. https://www.ecmwf.int/en/newsletter/165/meteorology/how-make-use-weather-regimes-extended-range-predictions-europe, last accessed: 21.10.2023) which could be likewise used to forecast the potential of wind energy production (Grams et al. 2017). We also note that other methods exist (and might be developed in future) that calculate WRs based on only 4 leading EOFs (e.g. Ferranti et al. 2014).

It has been suggested that MHWs can significantly affect marine ecosystems (Smale et al. 2019). The Baltic Sea can be considered exemplary for marginal seas with estuarine character to showcase such effects. Direct impacts of MHWs in the Baltic Sea were observed during the recent summer MHW 2018. Anomalous high temperatures up to 21 °C were registered in coastal bottom waters that likely led to increased emissions of carbon dioxide and methane (Humborg et al. 2019). Near to medium term forecasts of MHWs would also be desirable as the life cycle of many marine organisms is linked to the water temperature and consequently, anomalous high temperatures may negatively affect the marine ecosystems. For example, it has been reported that anomalous warm winter temperatures can considerably weaken the reproduction of western Baltic Herring (Polte et al. 2021). Another prominent example is harmful cyanobacteria blooms in the Baltic Sea, the likelihood of which to develop increases with warmer temperatures (Neumann et al. 2012; Meier et al. 2017). These blooms are a threat in many aspects as they negatively affect the water quality and so can negatively affect human recreation and aquaculture near the coasts, and stimulate oxygen deficiency in the open sea (Neumann et al. 2012). Currently, climate services to early detect such blooms are developed mainly employing real time satellite data and trend analysis at monitoring sites (Karlson et al. 2022), though these forecasts remain short term.

Finally, in the context of ongoing global climate warming, it is difficult to assess whether WRs will be equally important for MHWs in future climate as for the historical period. Taking the historical climate as a baseline to categorize MHWs, it is fairly likely that due to the thermodynamic climate response to greenhouse gases, which results in rising average water temperature, WRs will become less important. That means MHWs in the Baltic Sea will likely become independent from WRs because future mean temperatures come closer to the extremes diagnosed from the historical climate. However, climate models that are used to project global climate change in the framework of the Coupled Model Intercomparison Project should be tested if they can reproduce the relationship between WRs and MHWs as revealed by the hindcast simulation used in this study. This should be analyzed for other marginal seas as well since the relationship between atmospheric conditions and MHWs will likely be different in other regions of the world ocean.

Declarations

References

Balmaseda MA, Mogensen K, Weaver AT (2013) Evaluation of the ecmwf ocean reanalysis system oras4. Q J R Meteorol Soc 139(674):1132–1161

Beger M, Sommer B, Harrison PL, Smith SD, Pandolfi JM (2014) Conserving potential coral reef refuges at high latitudes. Divers Distrib 20(3):245–257

Behrens E, Rickard G, Rosier S, Williams J, Morgenstern O, Stone D (2022) Projections of future marine heatwaves for the oceans around New Zealand using New Zealand's earth system model. Front Clim 4:798287

Benthuysen JA, Oliver EC, Chen K, Wernberg T (2020) Advances in understanding marine heatwaves and their impacts. Front Mar Sci 7:147

Champeaux JL, Masson V, Chauvin F (2005) Ecoclimap: a global database of land surface parameters at 1 km resolution. Meteorol Appl 12(1):29–32

Christensen OB, Kjellström E, Dieterich C, Gröger M, Meier HEM (2022) Atmospheric regional climate projections for the Baltic Sea region until 2100. Earth Syst Dyn 13(1):133–157

Dee DP, Uppala SM, Simmons AJ, Berrisford P, Poli P, Kobayashi S, Andrae U, Balmaseda MA, Balsamo G, Bauer P, Bechtold P, Beljaars ACM, van de Berg L, Bidlot J, Bormann N, Delsol C, Dragani R, Fuentes M, Geer AJ, Haimberger L, Healy SB, Hersbach H, Hólm EV, Isaksen L, Kållberg P, Köhler M, Matricardi M, McNally AP, Monge-Sanz BM, Morcrette J-J, Park B-K, Peubey C, de Rosnay P, Tavolato C, Thépaut J-N, Vitart F (2011) The era-interim reanalysis: configuration and performance of the data assimilation system. Q J R Meteorol Soc 137(656):553–597

Dieterich C, Wang S, Schimanke S, Gröger M, Klein B, Hordoir R, Samuelsson P, Liu Y, Axell L, Höglund A, Meier HEM (2019) Surface heat budget over the north sea in climate change simulations. Atmosphere 10(5):272

Dutheil C, Meier HEM, Gröger M, Börgel F (2022) Understanding past and future sea surface temperature trends in the Baltic Sea. Clim Dyn 58(11):3021–3039

Dutheil C, Meier HEM, Gröger M, Börgel F (2023) Warming of Baltic Sea water masses since 1850. Clim Dyn 61(3):1311–1331

Elzahaby Y, Schaeffer A, Roughan M, Delaux S (2022) Why the mixed layer depth matters when diagnosing marine heatwave drivers using a heat budget approach. Front Clim 4:838017

Fereday D (2017) How persistent are north Atlantic–European sector weather regimes? J Clim 30(7):2381–2394

Ferranti L, Corti S, Janousek M (2014) Flow-dependent verification of the ecmwf ensemble over the Euro-Atlantic sector. ECMWF Newsl, pp 34–38

Goebeler N, Norko A, Norko J (2022) Ninety years of coastal monitoring reveals baseline and extreme ocean temperatures are increasing off the Finnish coast. Commun Earth Environ 3:215

Grams C, Beerli R, Pfenninger S, Staffell I, Wernli H (2017) Balancing Europe's wind power output through spatial deployment informed by weather regimes. Nat Clim Change 7:557–562

Gröger M, Dieterich C, Meier MHE, Schimanke S (2015) Thermal air-sea coupling in hindcast simulations for the North Sea and Baltic Sea on the NW European shelf. Tellus A: Dyn Meteorol Oceanogr 67(1):26911

Gröger M, Arneborg L, Dieterich C, Höglund A, Meier H (2019) Summer hydrographic changes in the Baltic Sea, Kattegat and Skagerrak projected in an ensemble of climate scenarios downscaled with a coupled regional ocean-sea ice-atmosphere model. Clim Dyn 53:5945–5966

Gröger M, Dieterich C, Meier H (2021) Is interactive air sea coupling relevant for simulating the future climate change of Europe? Clim Dyn 56(1):491–514

Gröger M, Dieterich C, Dutheil C, Meier HEM, Sein DV (2022a) Atmospheric rivers in cmip5 climate ensembles downscaled with a high-resolution regional climate model. Earth Syst Dyn 13(1):613–631

Gröger M, Placke M, Meier M, Börgel F, Brunnabend S-E, Dutheil C, Gräwe U, Hieronymus M, Neumann T, Radtke H, Schimanke S, Su J, Väli G (2022b) The Baltic Sea model inter-comparison project BMIP—a platform for model development, evaluation, and uncertainty assessment. Geosci Model Dev Discuss 2022:1–34

Hobday AJ, Alexander LV, Perkins SE, Smale DA, Straub SC, Oliver EC, Benthuysen JA, Burrows MT, Donat MG, Feng M et al (2016) A hierarchical approach to defining marine heatwaves. Prog Oceanogr 141:227–238

Hobday AJ, Oliver EC, Gupta AS, Benthuysen JA, Burrows MT, Donat MG, Holbrook NJ, Moore PJ, Thomsen MS, Wernberg T et al (2018) Categorizing and naming marine heatwaves. Oceanography 31(2):162–173

Hochman A, Messori G, Quinting JF, Pinto JG, Grams CM (2021) Do Atlantic–European weather regimes physically exist? Geophys Res Lett 48(20):e202109GL5574

Holbrook NJ, Scannell HA, Gupta A, Benthuysen JA, Feng M, Oliver EC, Alexander LV, Burrows MT, Donat MG, Hobday AJ et al (2019) A global assessment of marine heatwaves and their drivers. Nat Commun 10(1):1–13

Humborg C, Geibel MC, Sun X, McCrackin M, Mörth C-M, Stranne C, Jakobsson M, Gustafsson B, Sokolov A, Norkko A, Norkko J (2019) High emissions of carbon dioxide and methane from the coastal Baltic Sea at the end of a summer heat wave. Front Mar Sci 6:493

Huntington HP (2009) A preliminary assessment of threats to arctic marine mammals and their conservation in the coming decades. Mar Policy 33(1):77–82

Karlson B, Arneborg L, Johansson J, Linders J, Liu Y, Olofsson M (2022) A suggested climate service for cyanobacteria blooms in the Baltic Sea—comparing three monitoring methods. Harmful Algae 118:102291

Krapf K, Naumann M, Dutheil C, Meier HEM (2022) Investigating hypoxic and euxinic area changes based on various datasets from the Baltic Sea. Front Mar Sci. https://doi.org/10.3389/fmars.2022.823476

Kueh M, Lin C (2020) The 2018 summer heatwaves over northwestern Europe and its extended-range prediction. Sci Rep 10:19283

Li X, Donner SD (2022) Assessing future projections of warm-season marine heatwave characteristics with CMIP6 models. Earth Space Sci Open Arch, p 28

Madec G, Bourdallé-Badie R, Bouttier P-A, Bricaud C, Bruciaferri D, Calvert D, Chanut J, Clementi E, Coward A, Delrosso D et al (2017) Nemo ocean engine. Meteorol Appl

Meier H, Dieterich C, Eilola K, Gröger M, Höglund A, Radtke H, Saraiva S, Wåhlström I (2017) Future projections of record-breaking sea surface temperature and cyanobacteria bloom events in the Baltic Sea. Ambio 48(11):1362–1376

Meier M, Dieterich C, Gröger M (2021) Natural variability is a large source of uncertainty in future projections of hypoxia in the Baltic Sea. Commun Earth Environ 2:50

Meier HEM, Dieterich C, Gröger M, Dutheil C, Börgel F, Safonova K, Christensen OB, Kjellström E (2022a) Oceanographic

regional climate projections for the Baltic Sea until 2100. Earth Syst Dyn 13(1):159–199

Meier HEM, Kniebusch M, Dieterich C, Gröger M, Zorita E, Elmgren R, Myrberg K, Ahola MP, Bartosova A, Bonsdorff E, Börgel F, Capell R, Carlén I, Carlund T, Carstensen J, Christensen OB, Dierschke V, Frauen C, Frederiksen M, Gaget E, Galatius A, Haapala JJ, Halkka A, Hugelius G, Hünicke B, Jaagus J, Jüssi M, Käyhkö J, Kirchner N, Kjellström E, Kulinski K, Lehmann A, Lindström G, May W, Miller PA, Mohrholz V, Müller-Karulis B, Pavón-Jordán D, Quante M, Reckermann M, Rutgersson A, Savchuk OP, Stendel M, Tuomi L, Viitasalo M, Weisse R, Zhang W (2022b) Climate change in the Baltic Sea region: a summary. Earth Syst Dyn 13(1):457–593

Möllmann C, Cormon X, Funk S, Otto S, Schmidt J, Schwermer H, Sguotti C, Voss R, Quaas M (2021) Tipping point realized in cod fishery. Sci Rep 11:14259

Neumann T, Eidola K, Gustafsson B, Müller-Karulis B, Kuznetsov I, Meier H, Savchuk O (2012) Extremes of temperature, oxygen and blooms in the Baltic Sea in a changing climate. Ambio 41:574–585

Oliver EC, Donat MG, Burrows MT, Moore PJ, Smale DA, Alexander LV, Benthuysen JA, Feng M, Sen Gupta A, Hobday AJ et al (2018) Longer and more frequent marine heatwaves over the past century. Nat Commun 9(1):1–12

Polte P, Gröhsler T, Kotterba P, von Nordheim L, Moll D, Santos J, Rodriguez-Tress P, Zablotski Y, Zimmermann C (2021) Reduced reproductive success of western Baltic herring (Clupea harengus) as a response to warming winters. Front Mar Sci 8:10

Post E, Forchhammer MC, Bret-Harte MS, Callaghan TV, Christensen TR, Elberling B, Fox AD, Gilg O, Hik DS, Høye TT, Ims RA, Jeppesen E, Klein DR, Madsen J, McGuire AD, Rysgaard S, Schindler DE, Stirling I, Tamstorf MP, Tyler NJ, van der Wal R, Welker J, Wookey PA, Schmidt NM, Aastrup P (2009) Ecological dynamics across the arctic associated with recent climate change. Science 325(5946):1355–1358

Qiu Z, Qiao F, Jang CJ, Zhang L, Song Z (2021) Evaluation and projection of global marine heatwaves based on cmip6 models. Deep Sea Res Part II: Topical Stud Oceanogr 194:104998

Rantanen M, Karpechjko AY, Lipponen A, Nordling K, Hyvärinen O, Ruosteenoa K, Vihma T, Laaksonen A (2022) The arctic has warmed nearly four times faster than the globe since 1979. Commun Earth Environ 3:168

Receveur A, Bleil M, Funk S, Stötera S, Gräwe U, Naumann M, Dutheil C, Krumme U (2022) Western Baltic cod in distress: decline in energy reserves since 1977. ICES J Mar Sci 79(4):1187–1201

Samuelsson P, Jones C, Willén U, Ullerstig A, Gollvik S, Hansson U, Jansson C, Kjellström E, Nikulin G, Wyser K (2011) The Rossby Centre regional climate model rca3: model description and performance. Tellus A: Dyn Meteorol Oceanogr 63(1):4–23

Schulzweida U (2023) CDO user guide (2.3.0). Zenodo. https://doi.org/10.5281/zenodo.10020800

Smale DA, Wernberg T, Oliver ECJ, Thomsen M, Harvey BP, Straub SC, Burrows MT, Alexander LV, Benthuysen JA, Donat MG, Feng M, Hobday AJ, Holbrook NJ, Perkins-Kirkpatrick SE, Scannell HA, Sen Gupta A, Payne BL, Moore PJ (2019) Marine heatwaves threaten global biodiversity and the provision of ecosystem services. Nat Clim Change 9(4):306–312

Suursaar Ü (2020) Combined impact of summer heat waves and coastal upwelling in the Baltic Sea. Oceanologia 62(4, Part A):511–524

Vogt L, Burger FA, Griffies SM, Frölicher TL (2022) Local drivers of marine heatwaves: a global analysis with an earth system model. Front Clim 4:847995

Wåhlström I, Höglund A, Almroth-Rosell E, MacKenzie BR, Gröger M, Eilola K, Plikshs M, Andersson HC (2020) Combined climate change and nutrient load impacts on future habitats and eutrophication indicators in a eutrophic coastal sea. Limnol Oceanogr 65(9):2170–2187

Wåhlström I, Hammar L, Hume D, Pålsson J, Almroth-Rosell E, Dieterich C, Arneborg L, Gröger M, Mattsson M, Zillén Snowball L, Kågesten G, Törnqvist O, Breviere E, Brunnabend S-E, Jonsson PR (2022) Projected climate change impact on a coastal sea-as significant as all current pressures combined. Glob Change Biol 28(17):5310–5319